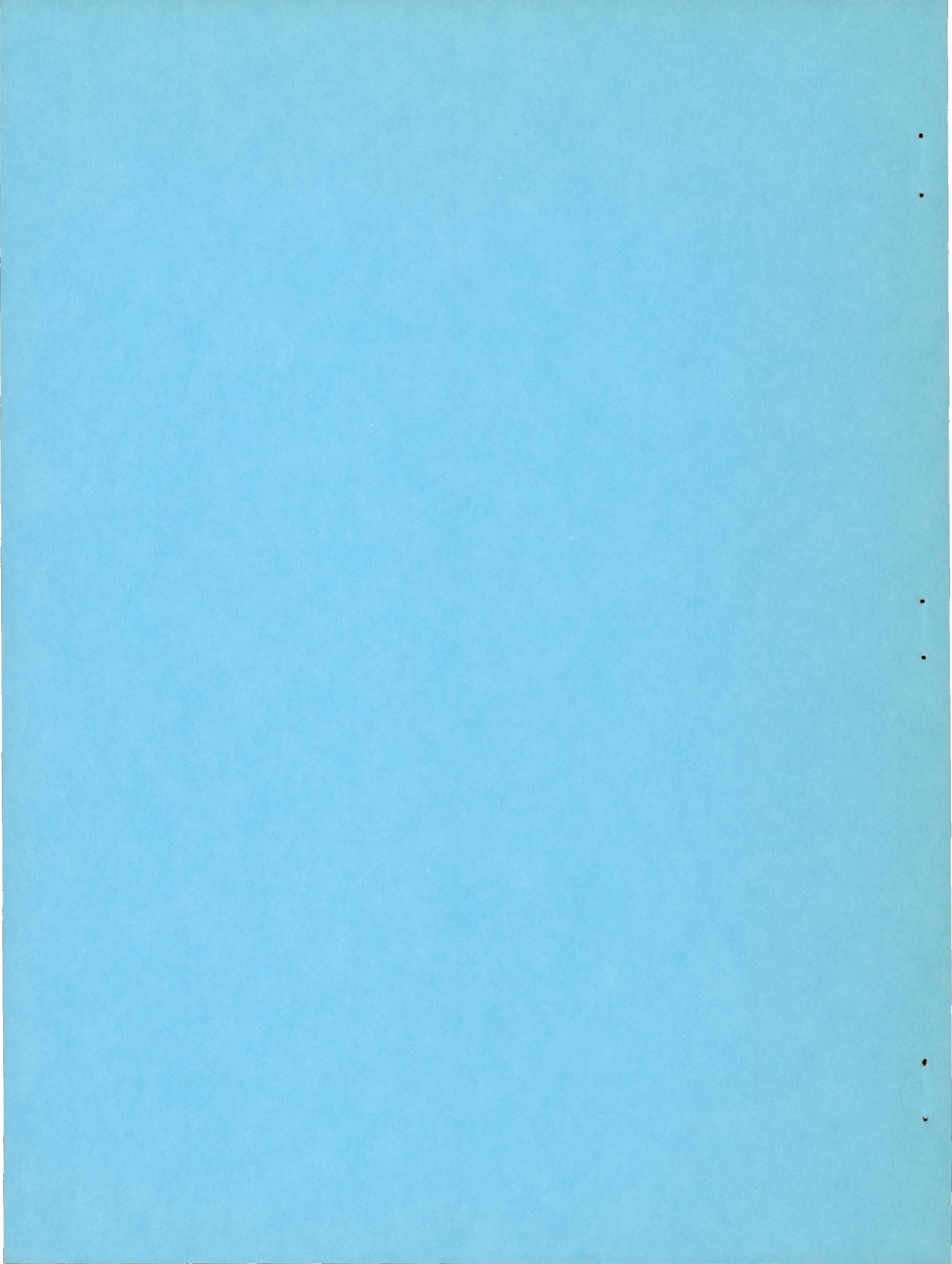# NACA

RESEARCH MEMORANDUM

PRELIMINARY INVESTIGATION OF A FIN-ACTUATED JET-VANE

CONTROL SYSTEM FOR STABILIZATION OF

ROCKET-POWERED MODELS

By Andrew R. Wineman

Langley Aeronautical Laboratory
Langley Field, Va.

NATIONAL ADVISORY COMMITTEE
FOR AERONAUTICS
WASHINGTON

NATIONAL ADVISORY COMMITTEE FOR AERONAUTICS

RESEARCH MEMORANDUM

PRELIMINARY INVESTIGATION OF A FIN-ACTUATED JET-VANE

CONTROL SYSTEM FOR STABILIZATION OF

ROCKET-POWERED MODELS

By Andrew R. Wineman

SUMMARY

Aerodynamic parameters and operation techniques were determined for a fin-actuated jet-vane system for the stabilization of a rocket-powered model by means of static and flight tests. Lift, hinge moment, and center-of-pressure location of the jet vane were obtained from a static test; while the longitudinal stability characteristics of a simplified flight model incorporating a fin-actuated jet-vane system were determined from the results of a flight test.

It was shown from the static test that the vane experienced small hinge moments and reasonably large lift forces and had a nearly constant center-of-pressure location. As a result of these characteristics, the flight model had favorable low-speed static stability shortly after take-off. Although oscillations in the pitch plane of the flight model were poorly damped, the damping of a pilotless-aircraft model-booster combination is expected to be greater than that of the model flown. Because of the complexity of the flow in the jet of the rocket, it was not possible to obtain close correlation between the experimental and theoretical values of vane lift coefficients, since the dynamic pressure and the Mach number of the jet could not be accurately calculated.

An additional flight test was made employing a powder-actuated separation unit to test this method of forcibly separating a flight model from its booster rocket. The operation of this unit was found to be satisfactory.

INTRODUCTION

The problem of stabilizing rocket-powered models and missiles during the boost period is of considerable importance due to the large booster-fin

area sometimes required. The feasibility of utilizing jet vanes for
stability and control has been discussed in references 1 and 2. It was
concluded from reference 1 that the application of jet vanes during the
boost period would provide a promising method of stabilization. It was
believed that a rocket-powered model utilizing a jet-vane control system
would reduce the large fixed fin area required for static stability.
This reduction of fin area would result in a decided decrease in drag
and an improvement in versatility and compactness of the booster.

The Pilotless Aircraft Research Division is conducting a series of
static and flight tests to determine the stability and control charac-
teristics of an immersed-type, jet-vane stabilization system. A simpli-
fied model employing a modified aircraft rocket motor and equipped with
internal vanes that were actuated by free-floating external fins was
tested and the results are presented and discussed in this paper.

Since the propulsion system of a free-flight model or missile may
be separable (two stage), the drag-weight ratios of the combination may
be such that the first stage would be difficult to separate from the
second stage. A check was made with a separate flight model incorporating
a powder-operated separation unit to test a method of forcibly separating
the first and second stages. The operation of this separation system is
also discussed herein.

SYMBOLS

C_L lift coefficient (L/qS)

L total lift of two vanes, pounds

H hinge moment, inch-pounds

M pitching moment about the center of gravity of the model,
             inch-pounds

F rocket thrust, pounds

a_n normal acceleration, positive upward, feet per second^2

g acceleration due to gravity, feet per second^2

$C_{L_{\delta_v}}$ rate of change of lift coefficient with vane deflection $(dC_L/d\delta_v)$,
             per degree

L_{δ_v} rate of change of lift with vane deflection $(dL/d\delta_v)$, pounds
             per degree

M_α rate of change of pitching moment with angle of attack $(dM/d\alpha)$, inch-pounds per degree

M_{δ_v} rate of change of pitching moment with vane deflection $(dM/d\delta_v)$, inch-pounds per degree

t time, seconds

α angle of attack, positive when the body axis is above the relative wind vector, degrees

δ_v jet-vane deflection, positive when trailing edge is down, degrees

δ_f floating-fin deflection, positive when trailing edge is up, degrees

l_v distance from center of gravity of model to hinge line of jet vane, inches

S vane area, two vanes, square feet

b vane span, feet

A aspect ratio, $\left(\dfrac{b^2}{S/2}\right)$

A_e cross-sectional area, square feet

I_Y moment of inertia of the model in pitch, slug-feet^2

P period of oscillation of the model in pitch, seconds

M Mach number

q dynamic pressure, pounds per square foot

p pressure, pounds per square foot

Subscripts:

f free-floating fin

v vane in rocket jet

e rocket nozzle exit

a   atmospheric

c   chamber

MODEL DESCRIPTION

The model used to test the jet-vane system in flight is shown in
figure 1. The jet vanes used were of the immersed cantilever type
having a low aspect ratio and hinged at 25 percent of the chord, as
shown in figure 2. They were constructed of an oil-hardening nonde-
forming die steel and were located at the nozzle exit. The vanes were
actuated through a mechanical system incorporating a 3:1 linkage ratio,
$\frac{\delta_v}{\delta_f} = 3$, by free-floating fins as shown in the schematic in figure 1(b).
The fins had a 45° delta plan form and were hinged at the leading edge
of the fin root section.

The flight model was controlled by a pair of jet vanes in the pitch
plane while two 45° delta fixed fins were used to stabilize the model in
the yaw plane. A photograph of the installation of the jet vanes in the
flight model is shown in figure 3. A modified 5-inch high-velocity air-
craft rocket equipped with a low thrust nozzle was used to propel the
model. A small pulse rocket, directed to produce a disturbing force in
the pitch plane, was mounted on top of the model approximately 16 inches
ahead of the center of gravity. The pulse rocket, normal accelerometer,
launching adapters, and wiring shields with symmetrical dummy shields
were all mounted externally on the rocket case without fairing. However,
the telemeter equipment and ballast were housed in an ogival nose section,
and the telemeter antenna was embedded in the leading edge of the fixed
fins.

Photographs showing the jet vanes mounted on a low thrust nozzle of
a 5-inch rocket motor before and after the static test are shown in fig-
ure 4. Modifications were made on the rocket grain and nozzle to change
the burning time and maximum thrust of the rocket motor. As shown in
figure 4(b), the condition of the vanes indicates that there was only a
small amount of erosion experienced during the static test.

INSTRUMENTATION

Strain-gage balances were employed in the static test to determine
thrust, lift, and vane hinge moment on a continuous time record in a
manner similar to that described in reference 3.

The flight model was equipped with a two-channel telemeter which transmitted a continuous time record of normal acceleration and vane deflection. The normal accelerometer was located near the center of gravity of the model, while the control position recorder was mounted on the exterior of the nozzle throat for compactness.

The trajectory, velocity, and longitudinal acceleration of the model were determined through the use of tracking radar and CW Doppler radar units. Radiosonde data were used to obtain density and the speed of sound throughout the altitude range traversed by the model.

TESTS

In order to determine the characteristics of the unconventional airfoil section of the vane, a static test was performed prior to the flight test. The static test also served as a proof test of the durability of the jet-vane system. Both jet vanes were fixed to simplify obtaining the hinge-moment data and were set at 15° to obtain the largest lift forces for negligible nozzle blocking effects. Prior to the firing, the angular deflections of the vanes under hinge moments were determined, and the value of 15° was corrected for the deflections that existed during the test.

The flight model was launched at an elevation of approximately 35° from a rail-type launcher. The low launching angle was chosen in the interest of range safety in the event of a stabilization-system failure. Information obtained from the flight was flight path, velocity, normal and longitudinal acceleration, and vane deflection.

RESULTS AND DISCUSSION

Static Test

Data obtained from the static test are presented in figures 5 and 6. The progressing thrust curve (increasing thrust with time), shown in figure 5, was a result of modifying the inhibitor of the propellant grain. The nozzle of the rocket motor was also modified from a standard multiple throat nozzle to a single-throat, low-thrust nozzle to accommodate installation of the jet vanes. Although this reduced the average thrust from approximately 5600 to 4300 pounds, the burning time of the standard rocket was increased from 0.88 to 1.13 seconds. Within the accuracy of the tests, the loss in impulse due to the drag of the vanes was negligible since the total impulse of the rocket motor with the vanes was equal to the total impulse of previously expended rocket motors having the same propellant grain.

Lift, hinge moment, center-of-pressure location, and deflection of the jet vane are shown in figure 6. The maximum lift and hinge moment experienced was approximately 162 pounds and 17 inch-pounds, respectively, while the center-of-pressure travel of the vane was from about 30 to 33 percent of the chord. Because of the hinge moments, the vanes deflected from the preset value of 15° to a value of slightly less than 13°. The variation of lift and hinge moments with time indicates that the flight model would be stable throughout the flight Mach number range, since the progressing lift curve and low hinge moments obtained from the static test are favorable conditions for a statically stable flight model. Since the hinge moments of the jet vane were small, it was possible to actuate the vanes with a free-floating fin system which was sensitive to angle of attack and therefore allowed angle-of-attack stabilization with this relatively simple system.

Flight Test

The variation of normal acceleration, vane deflection, and flight Mach number with time, for the power-on portion of the flight, is shown in figure 7. Throughout the flight Mach number range, $M = 0$ to $M = 1.15$, the recorded values of normal acceleration and vane deflection were never greater than $1.7g$ and 9°, respectively. Assuming the external fin was free-floating, a 9° maximum vane deflection would indicate a maximum angle of attack of approximately 3°.

Until the dynamic pressure over the external fin increased sufficiently to produce a hinge moment H_f equal to the hinge moment of the vane H_v which occurred at $t = 0.5$ second and was calculated to be 2.35 inch-pounds, the vane remained at a constant deflection and the external fin functioned as a fixed fin. However, when H_f increased to a value greater than 2.35 inch-pounds, due to the rapidly increasing dynamic pressure over the fin, the vane was actuated by the external fin. The larger the ratio of H_f/H_v the greater the tendency of the external fin to float freely and represent the angle of attack of the model. Before H_f became larger than H_v, an out of trim was apparent, $\delta_v = -3^\circ$ and $\frac{a_n}{g} = -0.5$, which was probably caused by erratic conditions within the nozzle at take-off. When the model had damped to a steady-state condition after burnout of the rocket motor, there was also an out of trim of approximately $\delta_v = -3.5^\circ$; however, the normal acceleration appeared to be trimmed near zero. This out of trim was attributed to antisymmetrical drag of the model, resulting from various external protrusions (launching fittings, accelerometer, and wiring shields) and was not related to the out of trim during the early part of the flight. At $t = 0.5$ second, when the dynamic pressure over the deflected external fin increased, the fin tended to return to $\alpha = 0$ and $\delta_v = 0$; therefore

the oscillations indicated in figure 7 were started. The pulse rocket, used as a disturbing force in pitch, hindered the existing oscillation by igniting out of phase, although the model continued to oscillate until burnout at slightly reduced amplitudes. The fact that the model experienced a finite oscillation during the flight indicated that the flight model was statically stable. The aerodynamic damping of the simple flight model was low because of the absence of lifting surfaces and because of the negligible body lift; therefore, low dynamic stability was indicated. It was assumed that the model had no body lift due to the various components attached to the exterior of the body and, therefore, did not contribute to model damping. The jet-vane system would contribute to total damping only if the actuating fin was not free-floating. If the jet-vane system were used to stabilize a two-stage or model-booster combination, the damping of the combination, and therefore its dynamic stability, would be greatly improved over the model flown.

A typical lift curve of the flight model at a flight Mach number range of $M = 0.88$ to $M = 0.94$ is shown in figure 8. The body of the model was very irregular (fig. 3); therefore it was assumed that the body contributed no lift to the total lift of the model. With the absence of wings or canards in the plane of the vanes the total lift, measured by the normal accelerometer and corrected for the varying propellant weight during power-on flight (see appendix), was attributed entirely to the jet vanes. Since the vane was in an expanding gas stream, lift curves were nonlinear for large vane angles; however, for vane angles less than 3° $(-3 < \delta_V < 3)$ it was possible to obtain lift curves (fig. 8). The slopes obtained from these curves, at various flight times, were plotted in figure 9. Only a limited number of slopes L_{δ_V} were obtained during the flight since lift curves for the first half-cycle and the half-cycle during which the pulse rocket fired were not used. For the angles that included linear lift curves, the values of L_{δ_V} progressively increased with flight time from 7 to 11 pounds per degree. These lift-curve slopes together with the corresponding values of periods of oscillation of the model (fig. 10) were used to obtain values of pitching moment per degree vane deflection M_{δ_V} by the two methods outlined in the appendix. Figure 11 is a plot of the variation of M_{δ_V} with flight time. The pitching moment per degree vane deflection obtained from equation (2) in the appendix compared favorably with M_{δ_V} obtained from equations (3) and (4). The test values of M_{δ_V} obtained by the two methods are grouped fairly close for a given flight time, this closeness indicating the accuracy of the stability, M_{δ_V}, and therefore M_{α}; and, therefore, a check on L_{δ_V} is provided.

Values of $C_{L_{\delta_V}}$ obtained from test values of L_{δ_V} by assuming a theoretical dynamic pressure over the vanes and by linearized theory are

plotted against flight time in figure 12. Although it is believed that
the test values of L_{δ_V} were fairly reliable, it was difficult to
express the lift-curve slope in a dimensionless coefficient $C_{L_{\delta_V}}$ since
test values of dynamic pressure at the vanes were not available.
Therefore, a theoretical value of dynamic pressure at the rocket nozzle
exit, obtained by equation (7) in the appendix, was employed in con-
junction with L_{δ_V} to obtain values of $C_{L_{\delta_V}}$, labeled as "flight test"
in figure 12. These values of dynamic pressure indicate an average
across the nozzle exit for an ideal nozzle when steady-state, adiabatic
conditions and perfect expansion are assumed. To compare $C_{L_{\delta_V}}$
obtained from L_{δ_V} with linearized theory, it was assumed that the jet
vanes were equivalent to a finite flat plate in a supersonic stream.
Then $C_{L_{\delta_V}}$ is a function of the jet Mach number and vane aspect ratio
as shown in equation (9) of the appendix. Since the vane is in at least
two regions of flow with different Mach numbers, the Mach number at the
nozzle exit and the Mach number when the jet is expanded to atmospheric
pressure, values of $C_{L_{\delta_V}}$ are presented for each Mach number (fig. 12).
The Mach number at the exit of the nozzle M_e is constant since it is a
function of the constant pressure ratio p_c/p_e and the nozzle geometry.
However, the Mach number obtained when the jet is expanded to atmospheric
pressure M_a is a function of the pressure ratio p_c/p_a which is
dependent upon the rocket thrust and atmospheric pressure. There is
very little change in theroetical $C_{L_{\delta_V}}$ by using the different Mach
numbers M_e and M_a. The values of $C_{L_{\delta_V}}$ obtained from L_{δ_V} are
from 0 to 25 percent higher than the theory indicates; however, it is
believed that a closer correlation between test and theory would be
obtained if the dynamic pressure and the jet Mach number over the vanes
could be determined accurately.

Separation Unit

The powder-operated separation unit, shown in figure 13, was tested
and found to be an adequate method of forcibly separating a flight model
from its booster.

The combustion chamber of the separation unit was attached to the
head of a 5-inch, light-weight, booster rocket while the multiple piston
arrangement was attached to a typical flight model having a 5-inch body
diameter. A 45-gram charge of FFFG black powder, ignited in the combustion
chamber by a delay squib, produced a pressure of approximately 2000 pounds
per square inch to force the smaller piston from its cylinder. The
remaining gas at reduced pressure forced the second, or larger, piston
from its cylinder to complete the separation. Rapid separation,

approximately 0.016 second, was realized when a 109-pound model was separated from an 83-pound booster in flight.

To insure a separation problem, the drag-weight ratio of the model was made greater than the drag-weight ratio of the booster. Premature separation was prevented by reducing the cross-sectional area of the first piston to the extent that the force produced would be less than the thrust of the booster prior to burnout.

If the drag-weight ratio of a flight model, or missile, is equal or greater than the drag-weight ratio of its booster, the usual drag separation method cannot be used; however, the model may be forcibly separated from the booster by employing a powder-operated separation unit.

CONCLUDING REMARKS

A simplified flight model has been successfully stabilized in one plane during the power-on portion of the flight by a fin-actuated jet-vane system.

Although the flight model had low aerodynamic damping due to the absence of lifting surfaces in the plane of the jet vanes, it would be reasonable to assume that the damping of a model-booster combination would be greatly improved in this respect. Because of the complexity of the flow in the jet of the rocket, it was not possible to obtain accurate values of dynamic pressure and Mach number over the vanes. The lift-curve slopes of the jet vanes $C_{L_{\delta_v}}$ obtained from the test values of L_{δ_v} and theoretical dynamic pressures were from 0 to 25 percent higher than $C_{L_{\delta_v}}$ obtained from linearized theory. To obtain closer correlation between test and theory, it would be necessary to determine accurately the dynamic pressure and Mach number over the vanes.

The application of a jet-vane system to a rocket booster may introduce a model-booster separation problem since the usual method of drag separation, which is generally employed with boosters having large fixed fins, would not apply in the case of low-drag boosters. To separate a flight model from a low-drag booster, an explosive-type separation unit, which demonstrated a rapid and clean method of forced separation, was flight tested.

Langley Aeronautical Laboratory
     National Advisory Committee for Aeronautics
         Langley Field, Va.

APPENDIX

COMPUTATION PROCEDURE

Jet-vane lift.- The lift on the model was corrected for the varying weight of the propellant grain in power-on flight by assuming that the weight of the expended propellant was proportional to the ratio of the impulse at a given time t and the total impulse of the rocket. The impulses were obtained from the approximate thrust curve in figure 5. This flight model thrust curve was estimated from data obtained from the static test and the burning time of the flight rocket motor. The burning time of the flight model, or the time at which maximum velocity occurred, was 1.80 seconds as determined by CW Doppler radar. With the use of these data, the variation of chamber pressure p_c with burning time and the thrust coefficient C_F of the rocket motor were obtained by a method similar to that described in reference 4. Therefore, the thrust of the flight model may be determined as a function of time since

$$F = C_F A_t p_c \tag{1}$$

where $p_c = f(t)$ and A_t is the cross-sectional area of the throat. A plot of thrust against time is shown as the estimated thrust of the flight model in figure 5. By taking the ratio of the area under the thrust curve at a given time to the total area, it was possible to obtain the weight of the expended fuel.

Model pitching moment.- The pitching moment about the model center of gravity due to vane deflection M_{δ_V} was obtained by two methods. The pitching moment per degree of vane deflection M_{δ_V} was determined from the product of L_{δ_V} and l_V and was also determined from the period of oscillation of the model. The distance from the vane hinge line to the model center of gravity was approximately 33.3 inches; therefore,

$$M_{\delta_V} = -l_V L_{\delta_V}$$

$$M_{\delta_V} = -33.3 L_{\delta_V} \tag{2}$$

From the solution of the equations of motion for two degrees of freedom, it was possible to express the stability of the model in terms of its damped natural frequency, moment of inertia, and damping by the equation:

$$M_\alpha = \frac{-I_Y}{57.3} (a^2 + b^2) \tag{3}$$

where $a = \frac{2\pi}{P}$ and b is the exponential damping coefficient in e^{-bt}. Since b^2 is about 1 percent of a^2, the damping term is neglected in the above equation. Because of the 3:1 mechanical gain between the jet vane and the free-floating fin, which functions as an angle-of-attack indicator, it is possible to obtain the following relation:

$$\delta_v = 3\alpha$$

$$M_{\delta_v} = \frac{1}{3} M_\alpha \tag{4}$$

Because of the mechanics of the linkage system (fig. 1), it was not possible to have a constant gain of 3:1 between the fin and the jet vane; however, the error introduced in equation (4) was small since the maximum angle of attack was about 3°. From equations (2) and (4), it was possible to obtain M_{δ_v} by two independent methods.

Theory.- To obtain $C_{L_{\delta_v}}$ from test values of L_{δ_v}, it was necessary to employ a theoretical expression for the dynamic pressure over the vanes. A relation for the dynamic pressure at the nozzle exit, obtained from reference 3, was assumed to apply over the vanes. This relation is

$$q_e = \frac{1}{2}\left[\frac{F}{A_e} - (p_e - p_a)\right] \tag{5}$$

Since the above equation assumes straight flow in the nozzle, a correction for nozzle divergence angle θ can be made by introducing the coefficient λ obtained from reference 5. This equation is

$$\lambda = \frac{1 - \cos 2\theta}{4(1 - \cos\theta)} \tag{6}$$

where θ is the divergence angle. In the case of the model flown $\lambda = 0.975$. Equation (5) may be expressed

$$q_e = \frac{1}{2\lambda}\left[\frac{F}{A_e} - (p_e - p_a)\right] \tag{7}$$

With the use of the values of dynamic pressure obtained from equation (7), it was possible to obtain values of $C_{L_{\delta_v}}$ by

$$C_{L_{\delta_v}} = \frac{L_{\delta_v}}{q_e S} \tag{8}$$

An expression for theoretical lift-curve slope of a flat plate of zero thickness in a supersonic stream (reference 6) was used to compare with $C_{L_{\delta_V}}$ from equation (8). This equation is

$$C_{L_{\delta_V}} = \frac{4}{\sqrt{M^2 - 1}} \left[1 - \frac{1}{2A\sqrt{M^2 - 1}} \right] \tag{9}$$

Thus the $C_{L_{\delta_V}}$ obtained by linearized theory is a function of jet Mach number and vane aspect ratio.

REFERENCES

1. Rosan, H. J.: LTV-N-4b1 (VTV-1) Design, Development, and Flight
     Test. CAL/CM-547, CAL-1-D-2, Cornell Aero. Lab., May 27, 1949.

2. Rose, C. H., and Immenshuh, W. T.: Report on Engineering Study and
     Investigation of the Problems of Jet-Thrust Systems As Related to
     Control of an Airplane. Pts. I and II. Rep. No. 3817-6, Ryan
     Aero. Co., April 28, 1948.

3. Bond, Aleck C.: Experimental Investigation of a Flat-Plate Paddle Jet
     Vane Operating on a Rocket Jet. NACA RM L50I20, 1950.

4. Purser, Paul E., Thibodaux, Joseph G., and Jackson, H. Herbert: Note
     on Some Observed Effects of Rocket-Motor Operation on the Base
     Pressures of Bodies in Free Flight. NACA RM L50I18, 1950.

5. Zucrow, M. J.: Principles of Jet Propulsion and Gas Turbines. John
     Wiley & Sons, Inc., 1948, p. 493.

6. Powell, W. B.: Experimental Investigations with Jet Control Vanes.
     Progress Rep. No. 4-30, Jet Propulsion Lab., C.I.T., 1948.

Telemeter section

Rocket motor

C.G. Location

Pulse rocket

Station
0

20.2   26.2   42.1   53.0   68.0   75.4

45°

Normal accelerometer
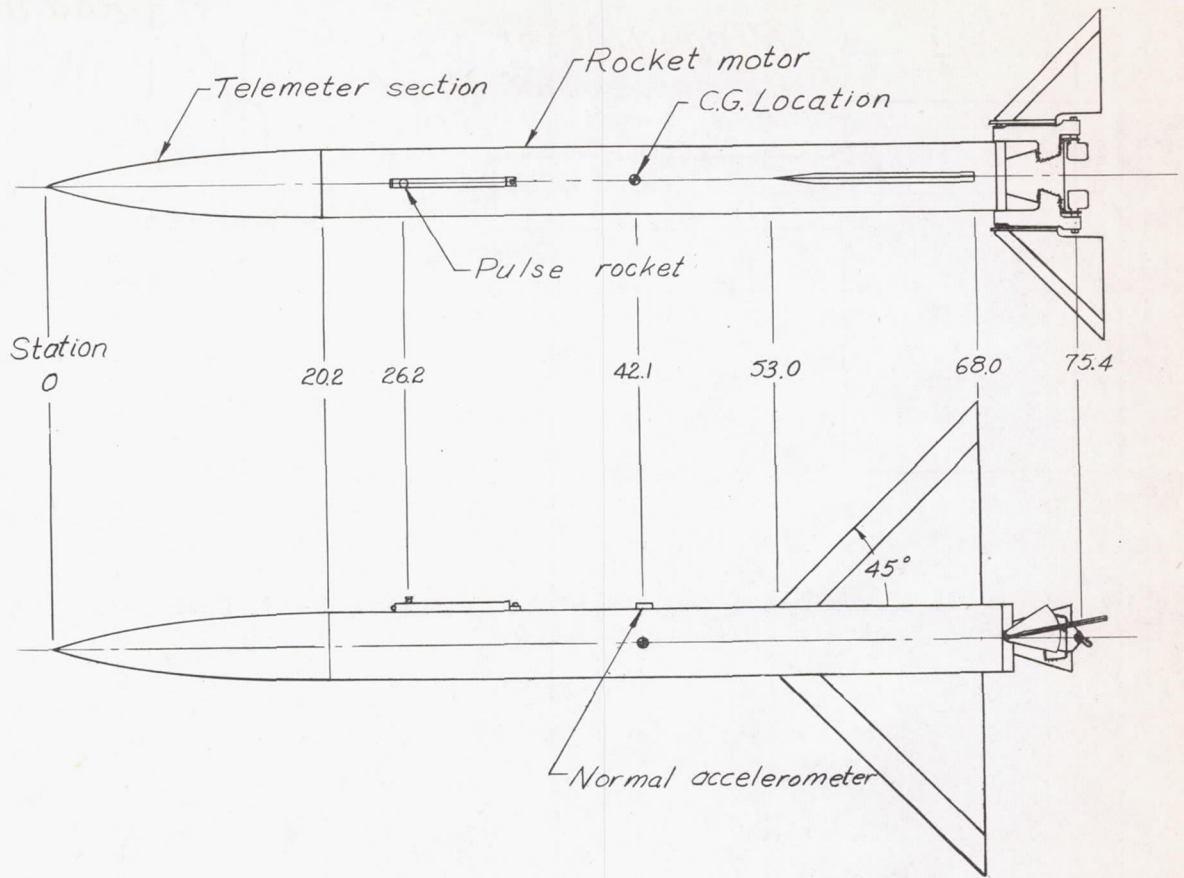
(a) Flight model. All dimensions in inches.

Fin pivot   Vane pivot

Free-floating fin

δ_f

$\delta_v = 3\delta_f$

Jet vane

NACA

Slide pivot

Relative
wind
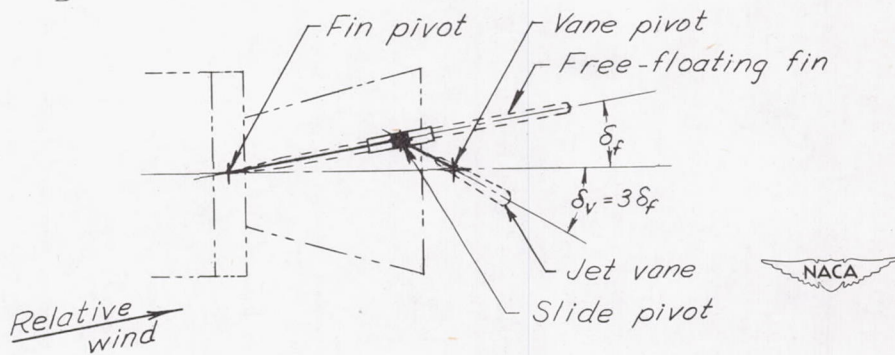
(b) Schematic of fin-vane linkage.

Figure 1.- General arrangement of flight model showing the jet-vane
linkage system.
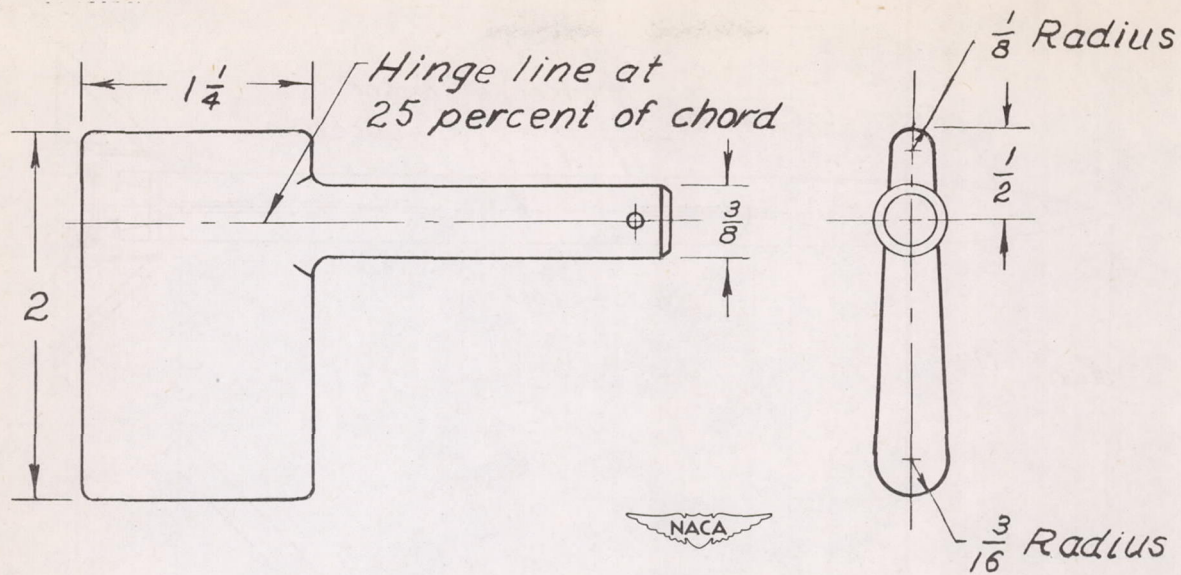
Figure 2.- Sketch of jet vane. All dimensions in inches.
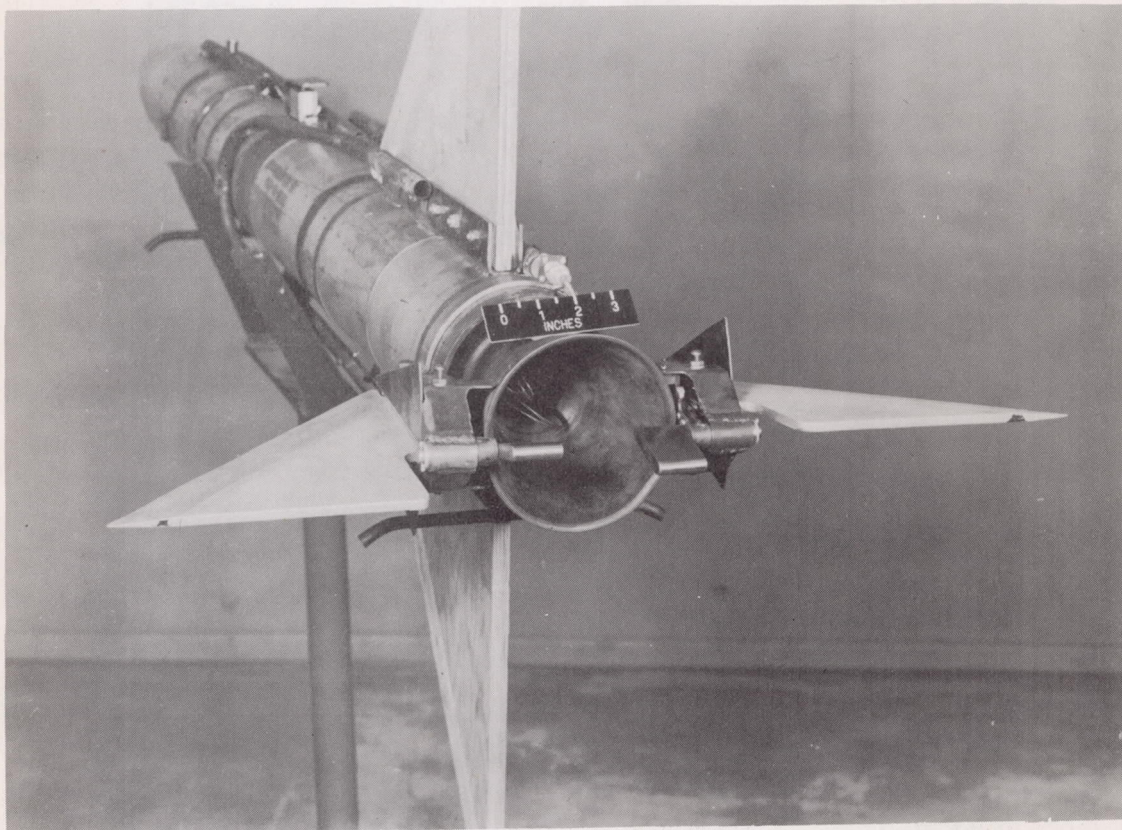
Figure 3.- Flight model showing jet vanes.
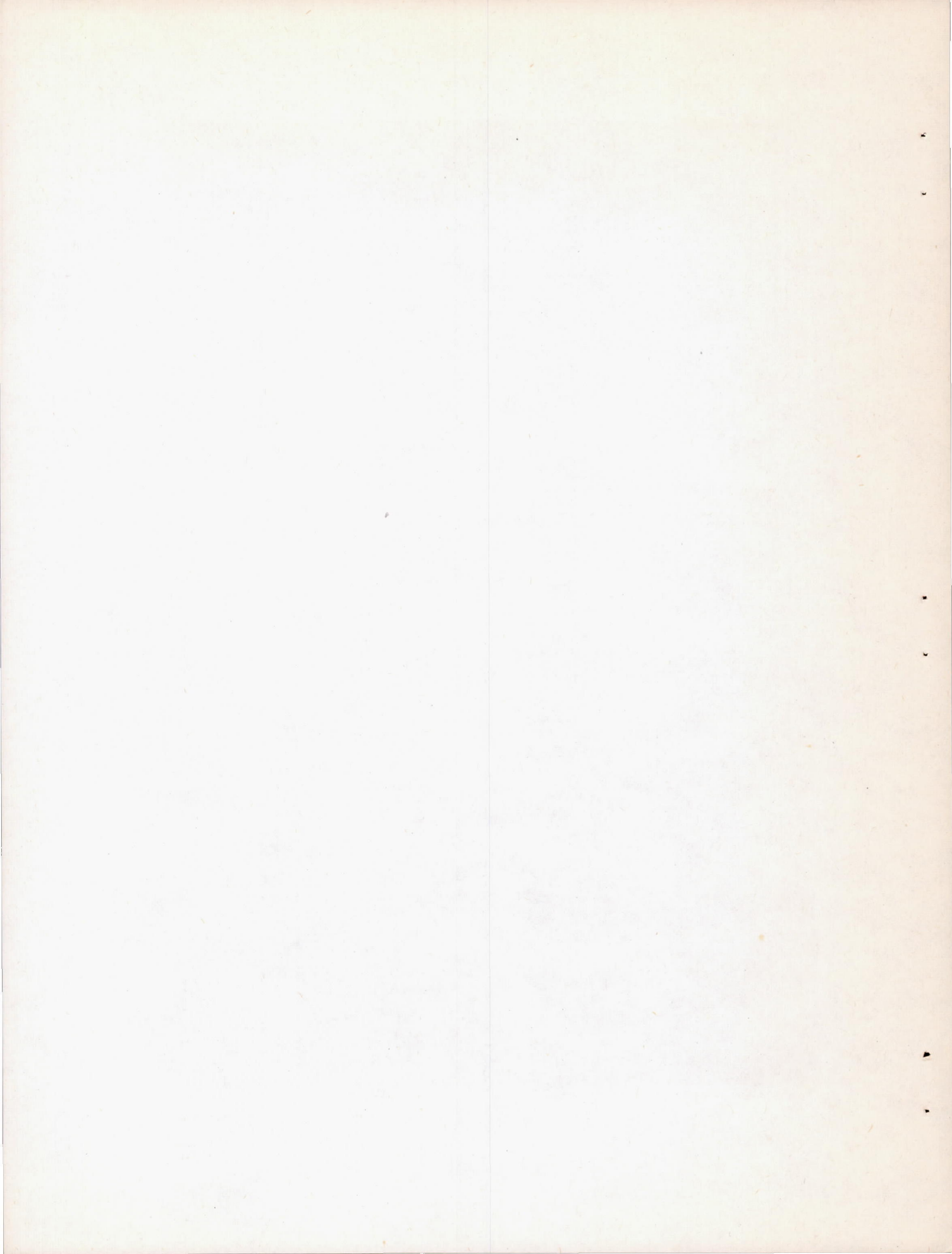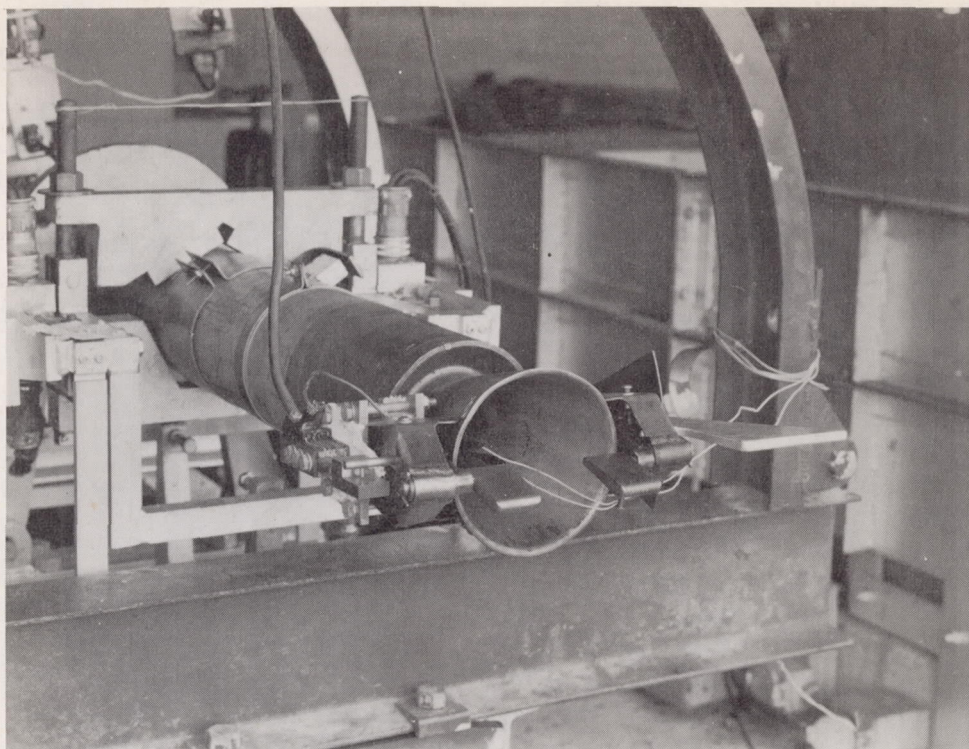
(a) Before firing.
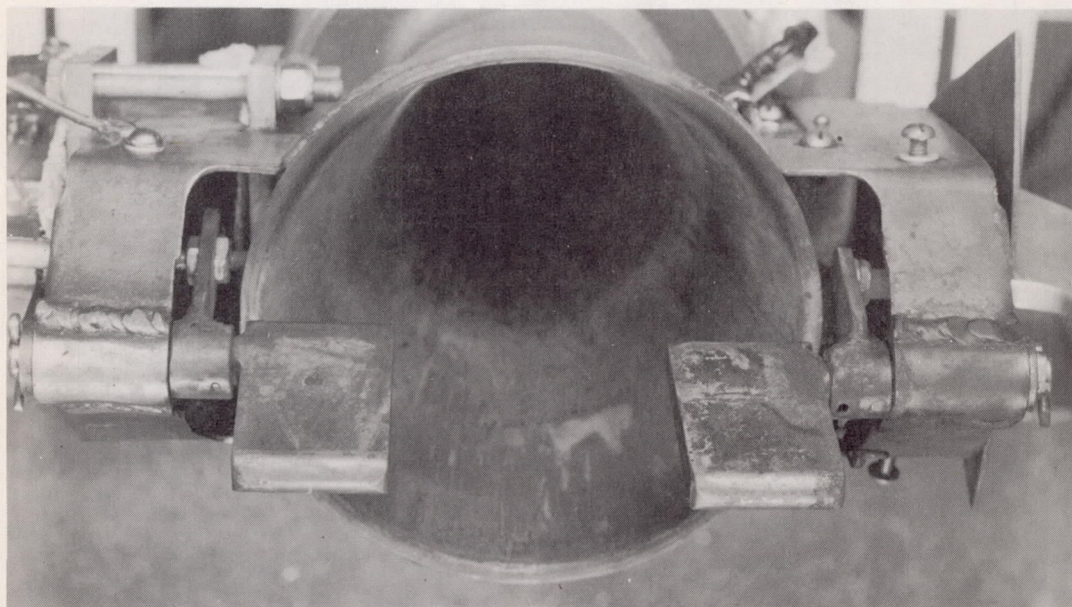
L-62535

(b) After firing.

Figure 4.- Static test of jet vanes.

L-62534
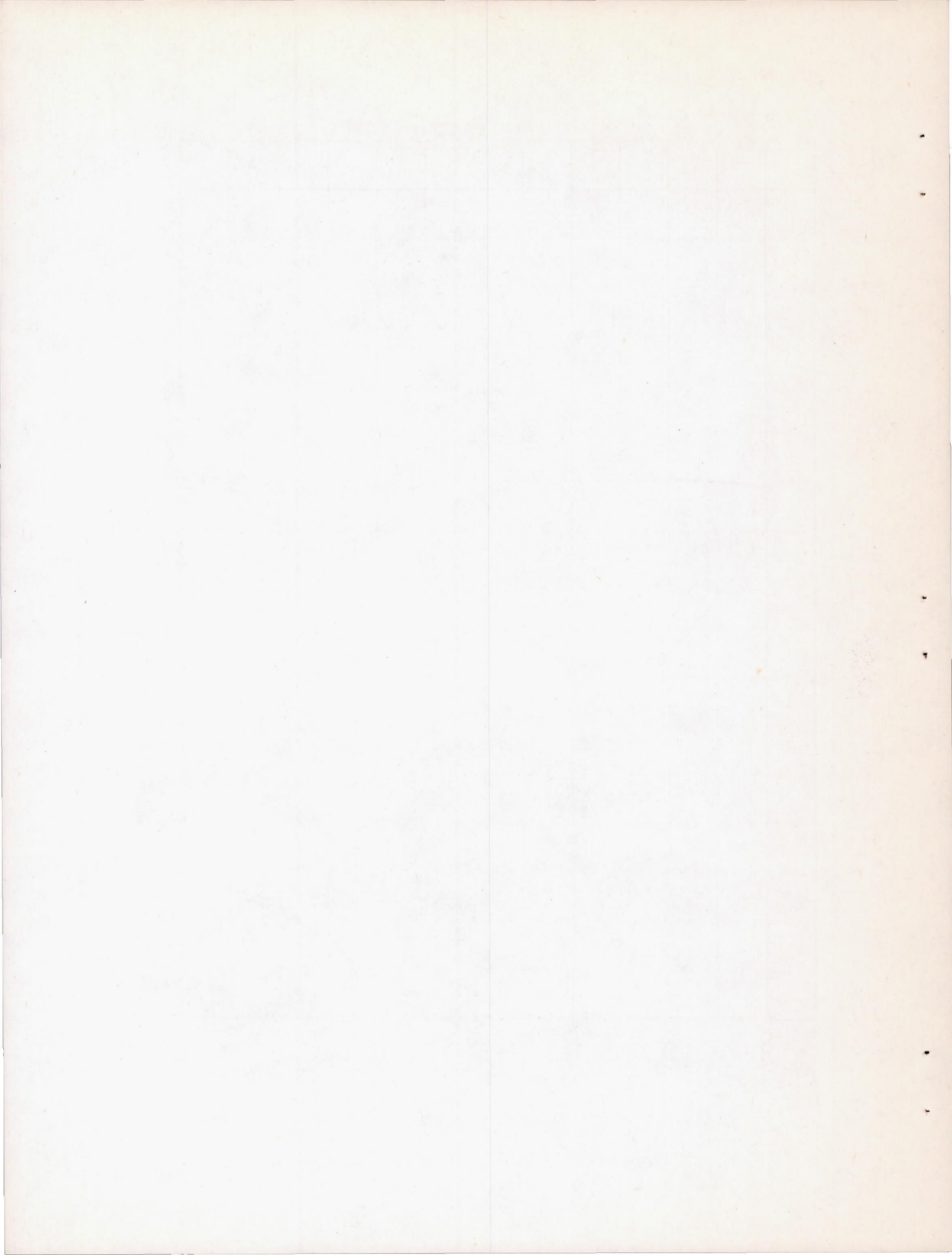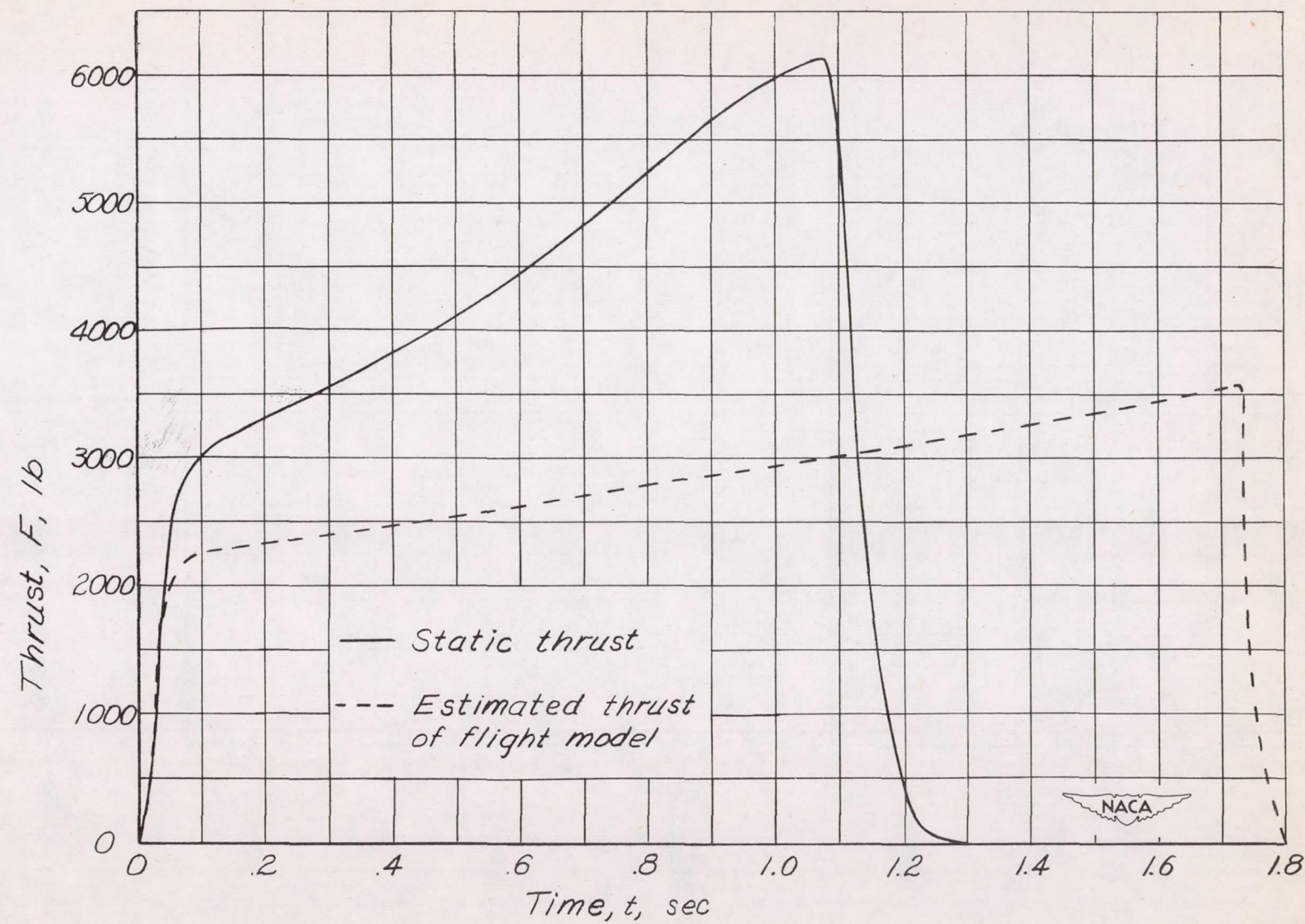
Figure 5.- Variation of thrust for static and flight tests.
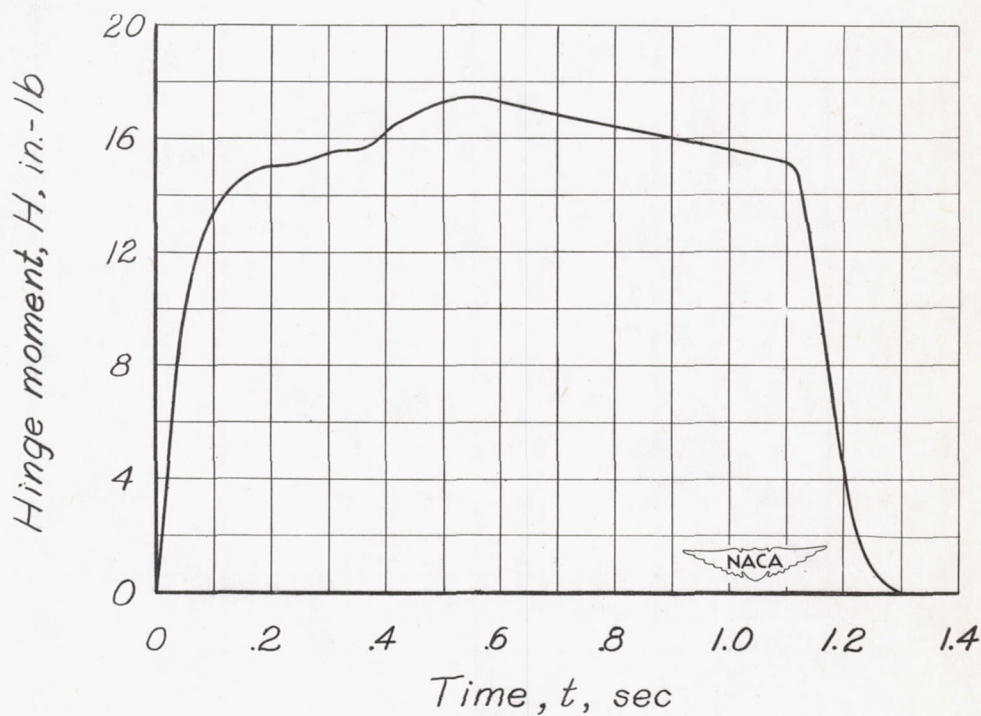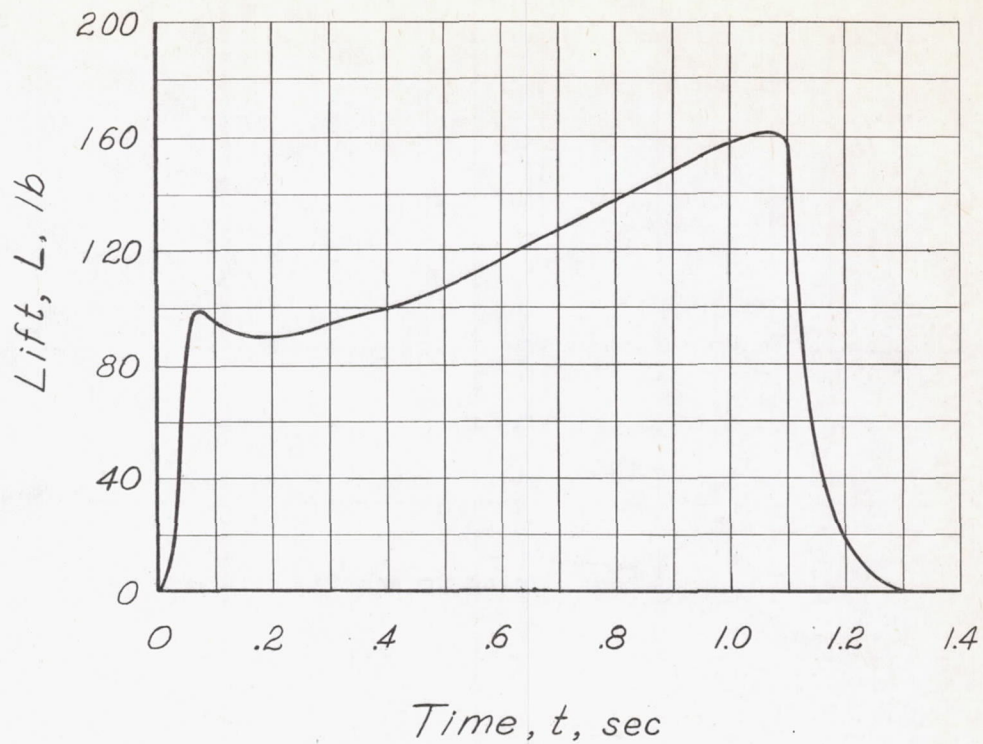
Figure 6.- Aerodynamic characteristics of vane from static test.
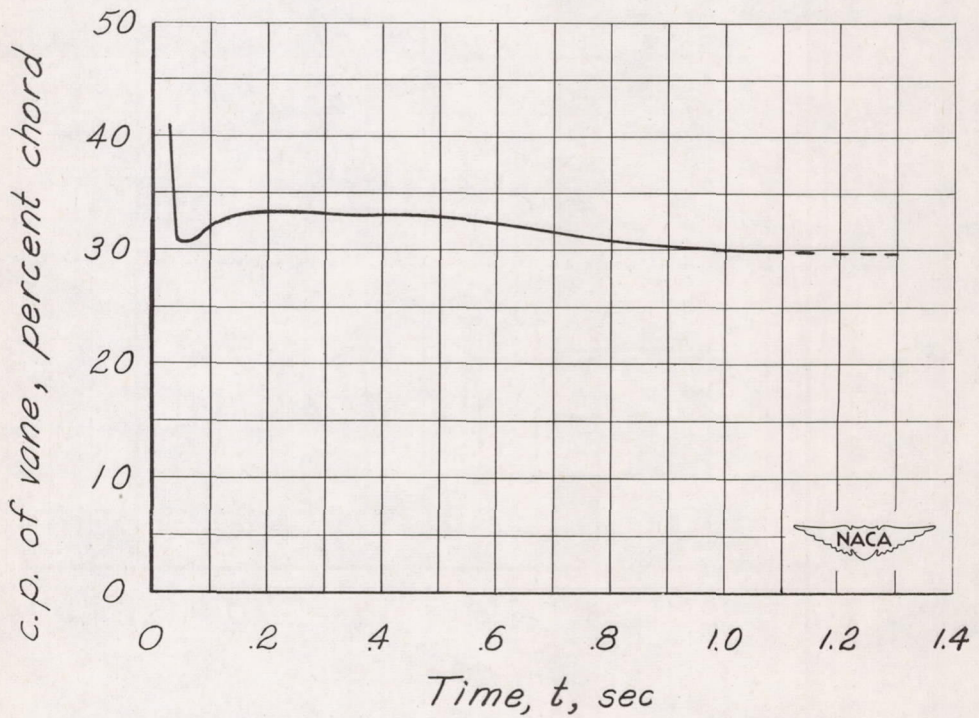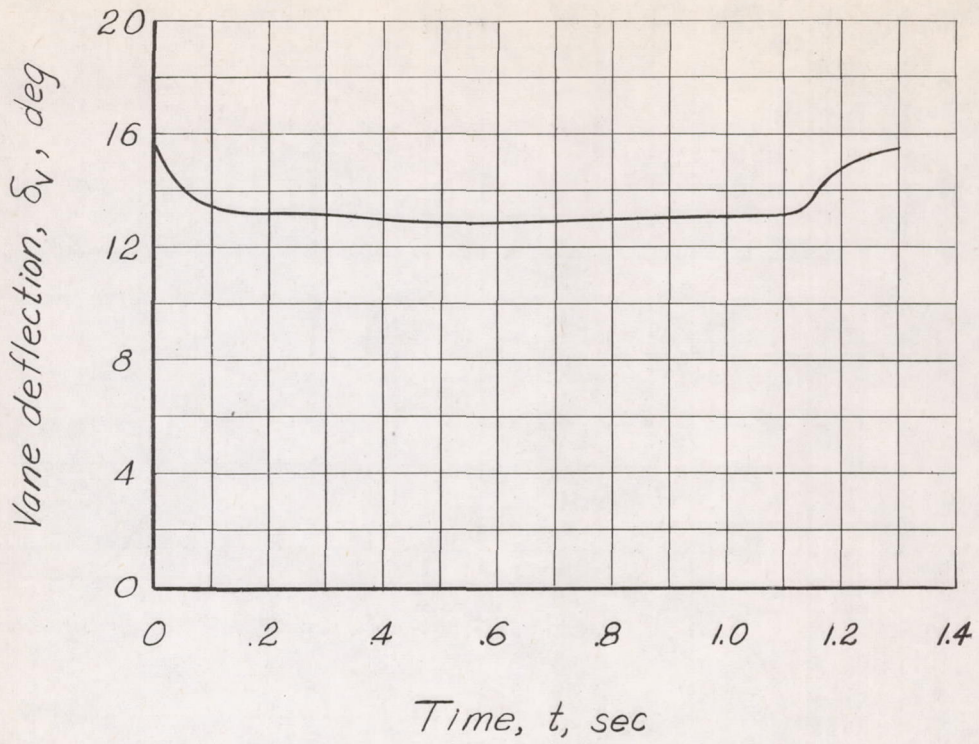
Figure 6.- Concluded.
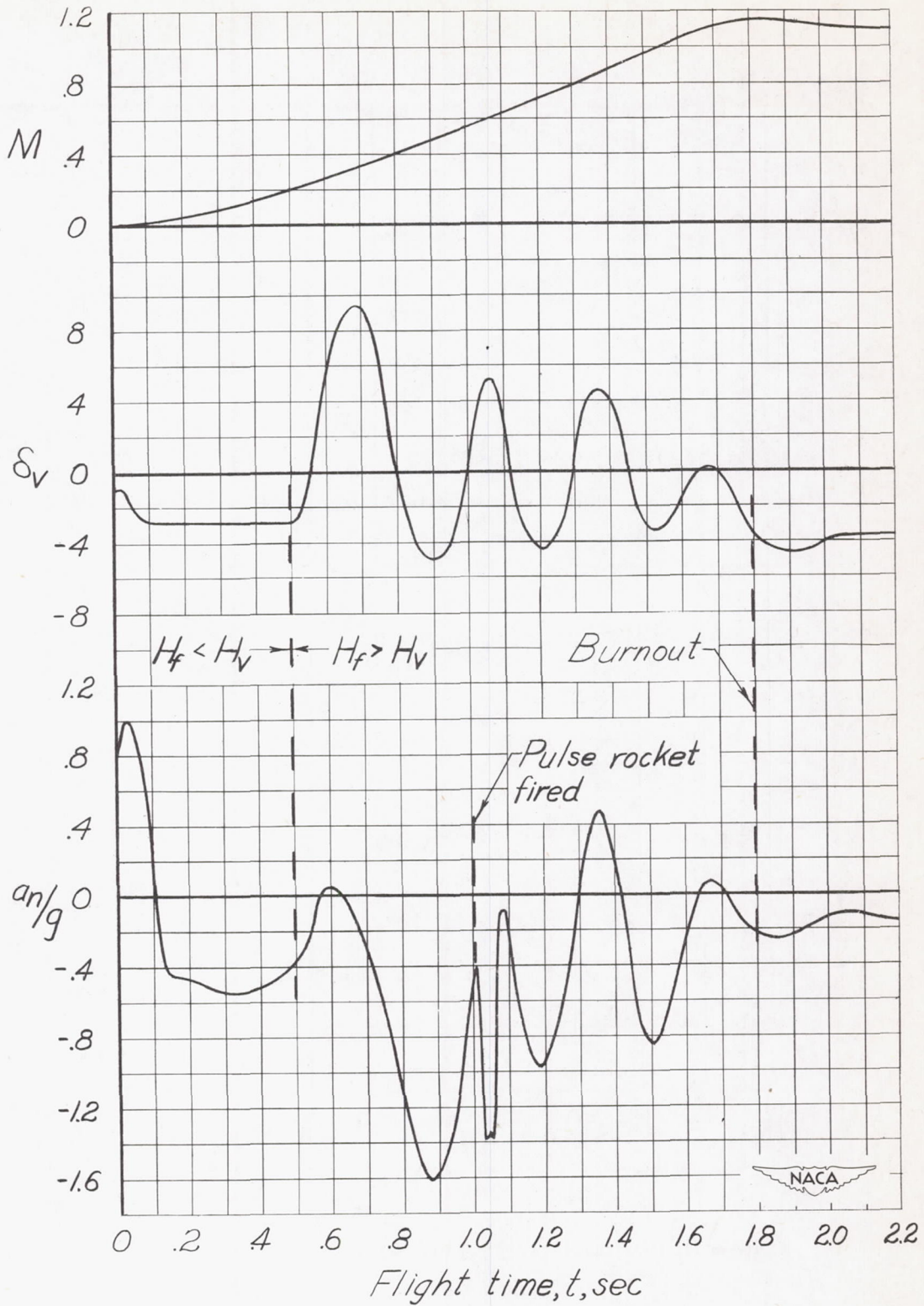
Figure 7.- Time history of flight model.
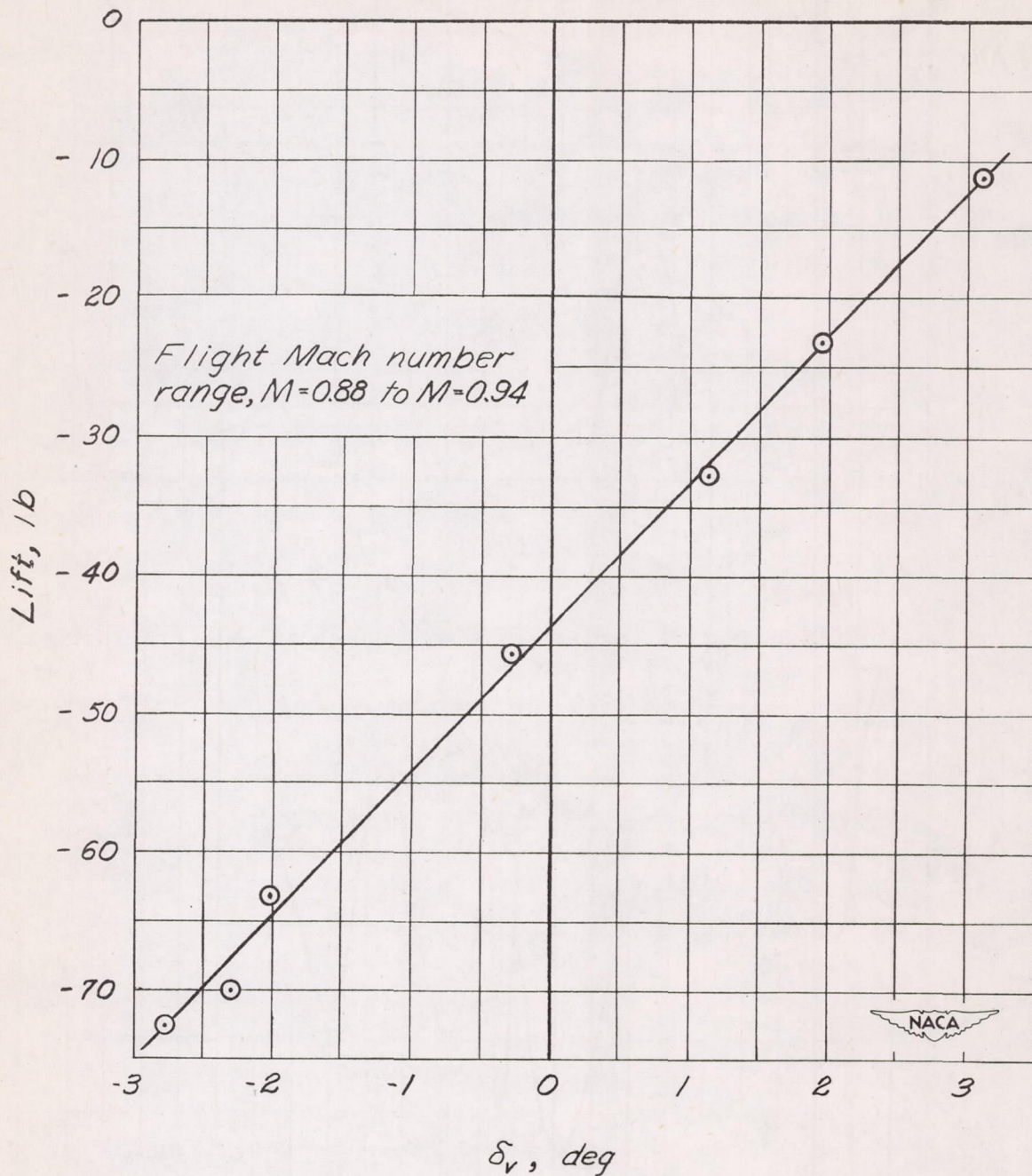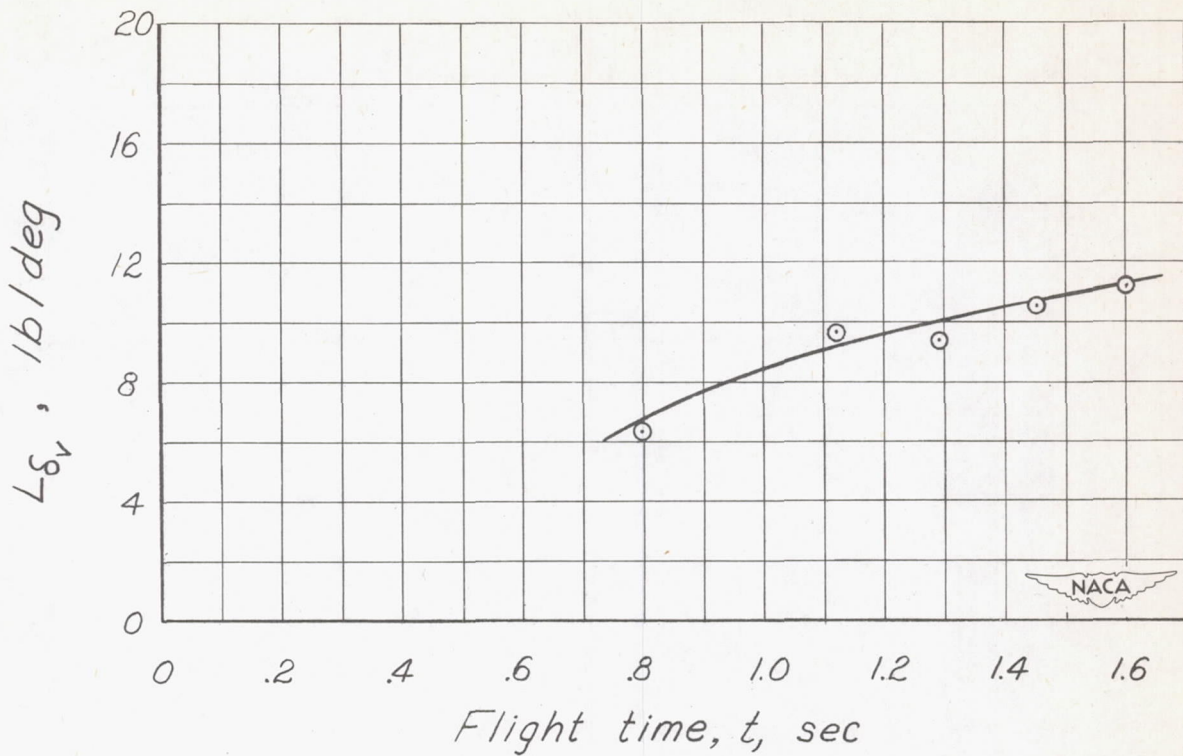
Figure 8.- Variation of lift with vane deflection.

Figure 9.- Variation of lift per degree vane deflection with flight time.
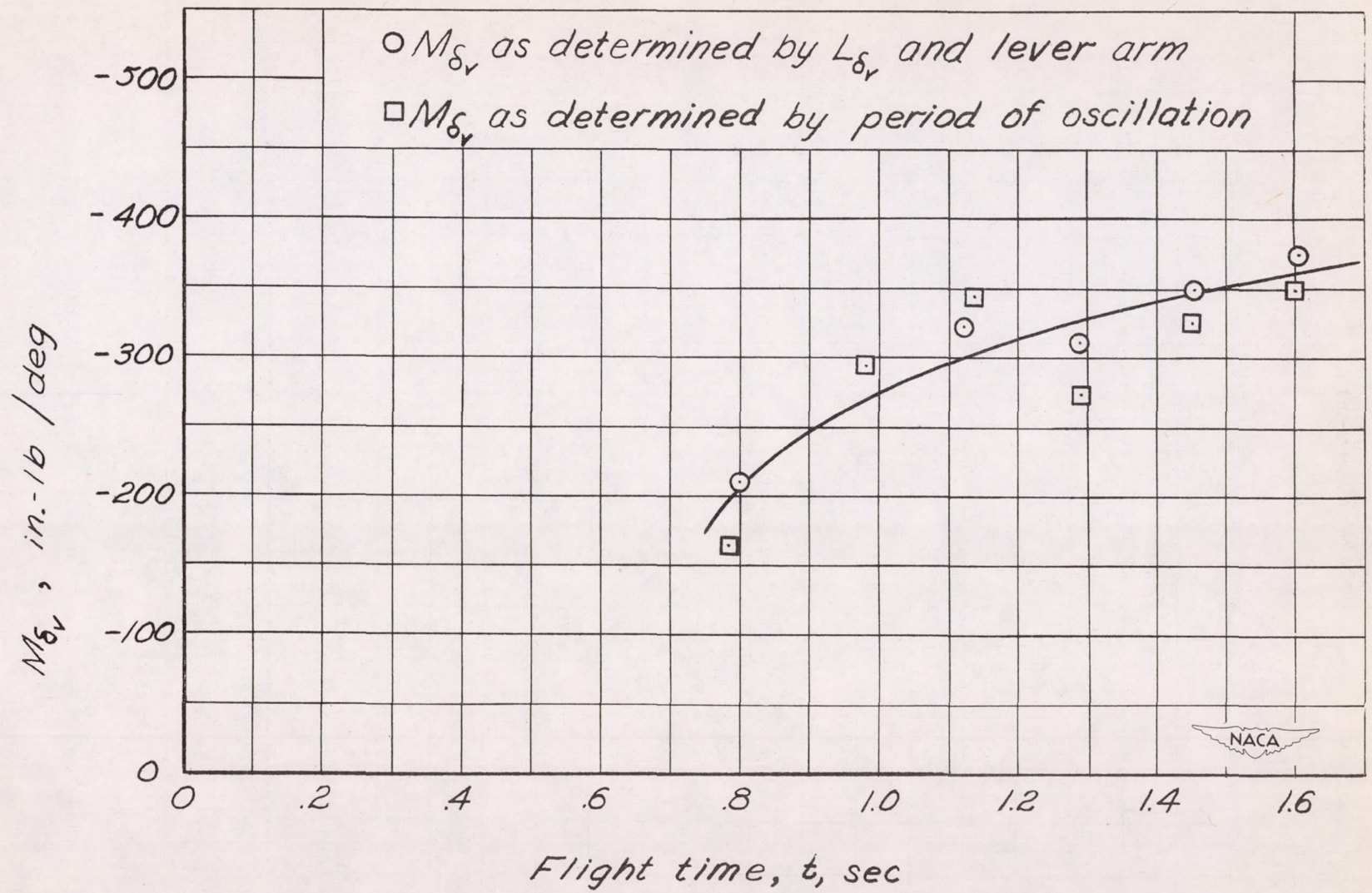(δ_V range $\pm 3^\circ$.)
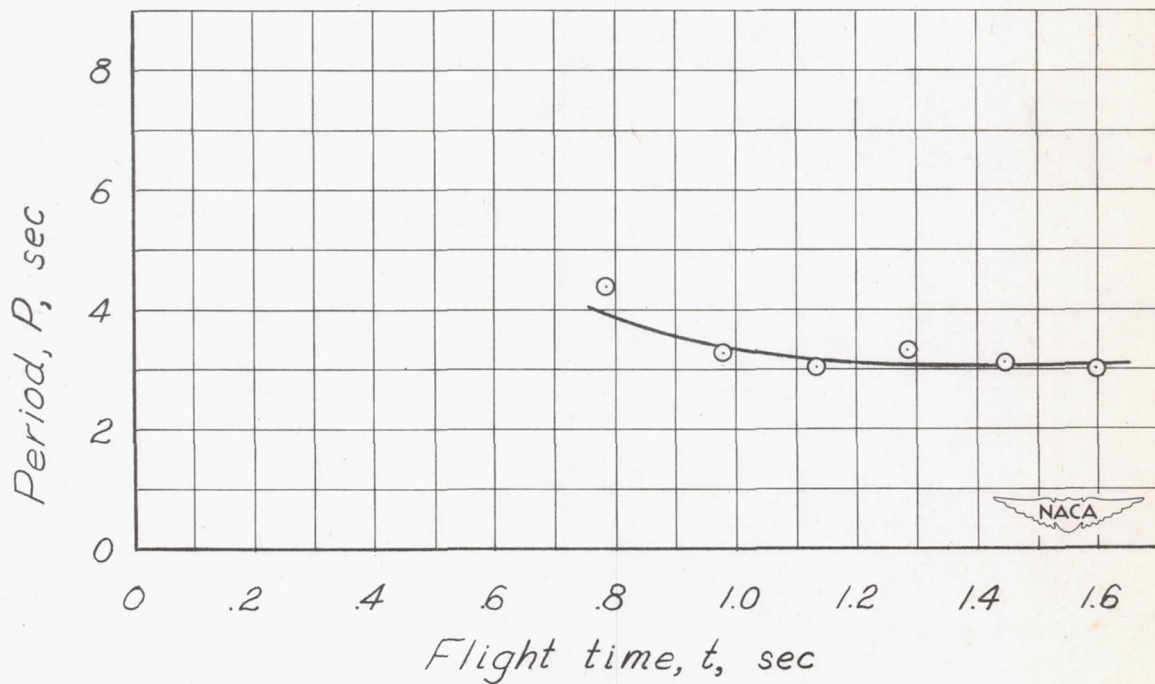
Figure 10.- Variation of model period with flight time.

Figure 11.- Variation of moment per degree vane deflection at model center of gravity with flight time.
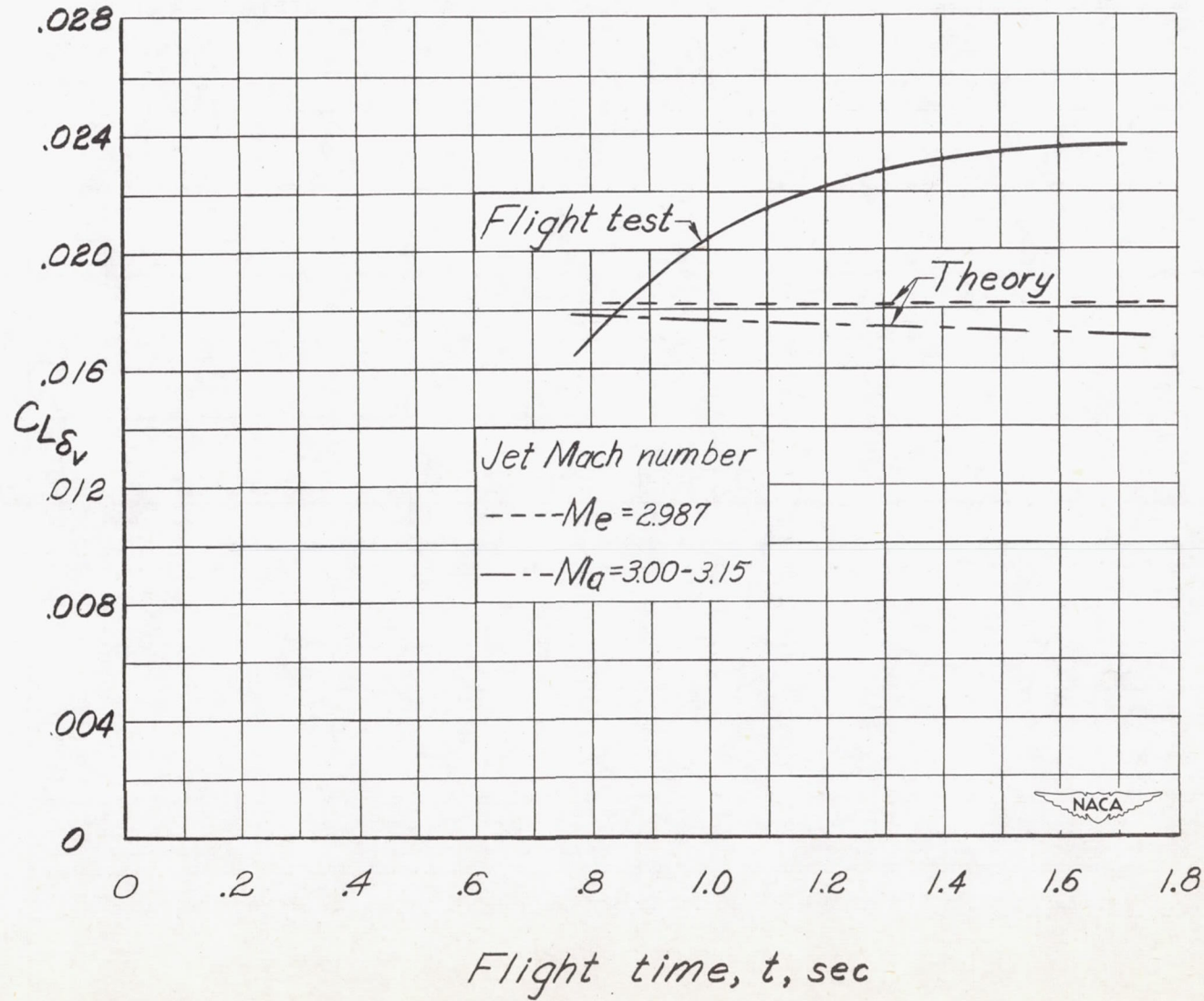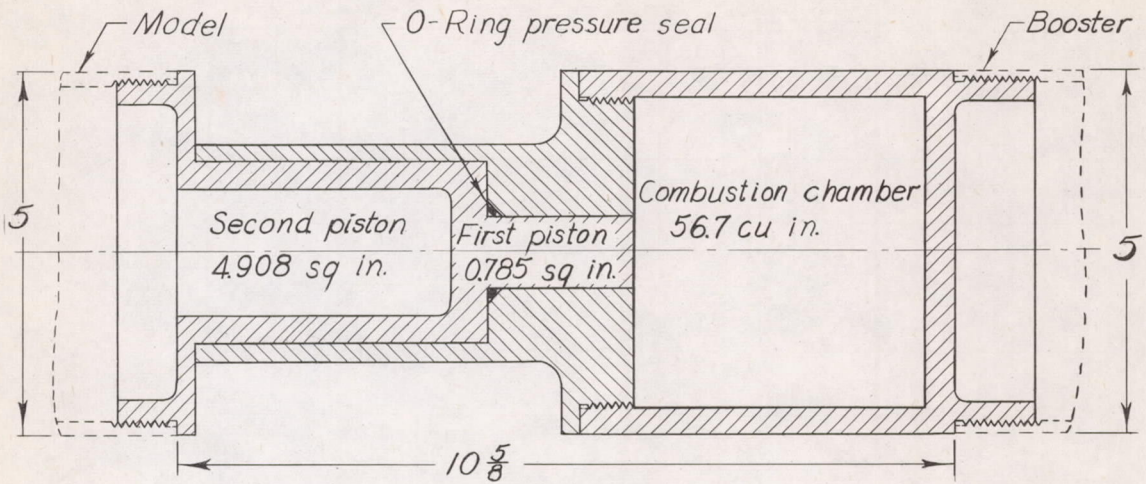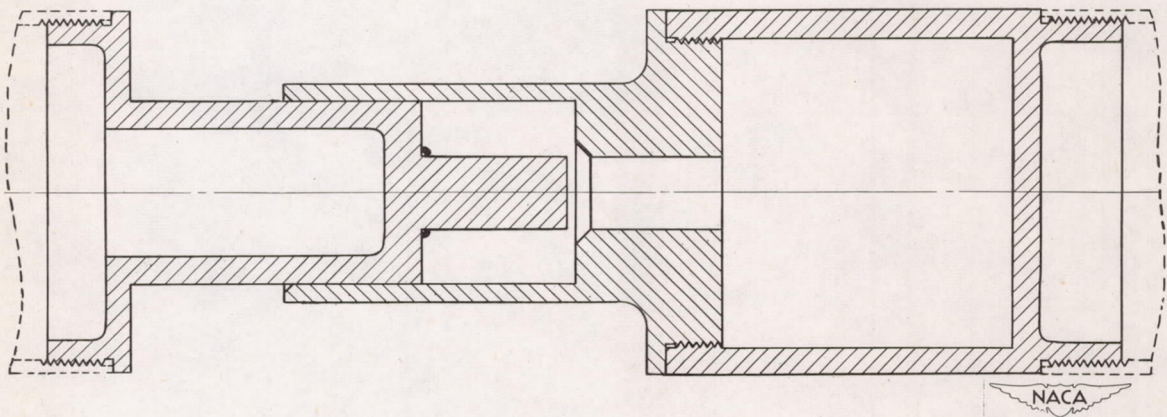
Figure 12.- Lift-curve slope of jet vane from flight test. (δ_v range $\pm 3°$.)

(a) Before separation.

(b) Partially separated.

Figure 13.- Booster separation unit. All dimensions in inches.